

M. Bottini,^{a,b} M. C. Yadav,^b K. Bhattacharya,^c A. Magrini,^a N. Rosato,^a B. Fadeel,^c C. Farquharson,^d and J. L. Millán^b

^aNAST Centre and Department of Experimental Medicine and Surgery, University of Rome Tor Vergata; ^bSanford Burnham Prebys Medical Discovery Institute, La Jolla, US; ^cKarolinska Institutet, Stockholm, Sweden; ^dThe University of Edinburgh, Midlothian, Scotland, UK

BACKGROUND

- Matrix vesicles (MVs) are a special class of extracellular vesicles (EVs) that initiate mineralization in cartilage and other vertebrate tissues by accumulating Ca^{2+} and inorganic phosphate (P_i) and forming crystalline mineral deposits.¹
- During the first stages of mineralization, mineral deposits of Ca^{2+} and P_i within the MV lumen are not crystalline and form the so called nucleation core (NC).²
- We have recently shown that MV calcification is regulated by PHOSPHO1. The genetic ablation of *Phospho1* impairs the formation of mineral deposits within the MV lumen, suggesting that intra-vesicular production of P_i is necessary for the correct $\text{Ca}^{2+}/\text{P}_i$ stoichiometry for NC formation.³

OBJECTIVE

- Investigate the role of PHOSPHO1 on MV biogenesis and volume growth.
- Monitor the mineralization status of MVs with differing mineralization potential, i.e. mineralization-competent (WT) and mineralization-compromised (*Phospho1*^{-/-}) MVs.

METHODS

- Tapping-mode AFM (TM-AFM) topography imaging under light tapping has been used to characterize the volume and number of WT and *Phospho1*^{-/-} MVs.
- TM-AFM phase imaging under inelastic cantilevered tip-sample interactions has been used to map elastic property variation in WT and *Phospho1*^{-/-} MVs and enable compositional mapping.

RESULTS

- WT and *Phospho1*^{-/-} MVs appeared as globular flattened features (Figure 1A). The number of WT MVs was statistically greater than the number of *Phospho1*^{-/-} MVs (Figure 1B). WT MVs had a left-skewed volume distribution with mode and mean value of $11 \times 10^3 \text{ nm}^3$ and $22 \times 10^3 \text{ nm}^3$, respectively, whereas the distribution of volumes for *Phospho1*^{-/-} MVs had a narrow distribution with both mode and mean value of $10 \times 10^3 \text{ nm}^3$ (Figure 1C).
- WT MVs showed changes in surface morphology and phase with vesicle volume (Figure 2). Phase distribution showed the presence of a portion of MV lumen stiffer than other portions. We posit that this portion is the NC.
- The portion of WT MV lumen surrounding the NC was composed by two parts: one was less stiff than other vesicle portions, the other had values of stiffness lower than the NC and formed clusters around the NC within bigger vesicles.
- Phospho1*^{-/-} MVs did not show any appreciable changes in surface morphology and phase with changes in vesicle volume.

CONCLUSIONS

- AFM topography and phase imaging enabled us to track the changes in the lumen of WT and *Phospho1*^{-/-} MVs and validate the role of PHOSPHO1 in regulating the intra-vesicular level of P_i necessary to trigger NC formation.
- Future studies will aim at relating compositional variation in MV lumina to vesicle nanoscale elastic modulus. These studies will use a combination of Raman spectroscopy and AFM nano-indentation on volume-fractionated MVs.

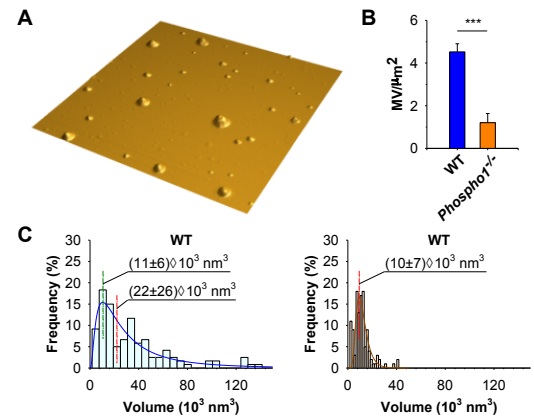


Figure 1. Morphology, number and volume distribution of WT and *Phospho1*^{-/-} MVs. A. TM-AFM 3D topography images of WT MVs. Scan size $3 \mu\text{m} \times 3 \mu\text{m}$. B. Number of WT and *Phospho1*^{-/-} MVs in a scan size with an area of $1 \mu\text{m}^2$. Results are expressed as mean \pm SEM. Statistical differences between samples were calculated by non-parametric Mann-Whitney U analysis. *** $p < 0.001$. C. Volume distribution for WT and *Phospho1*^{-/-} MVs.

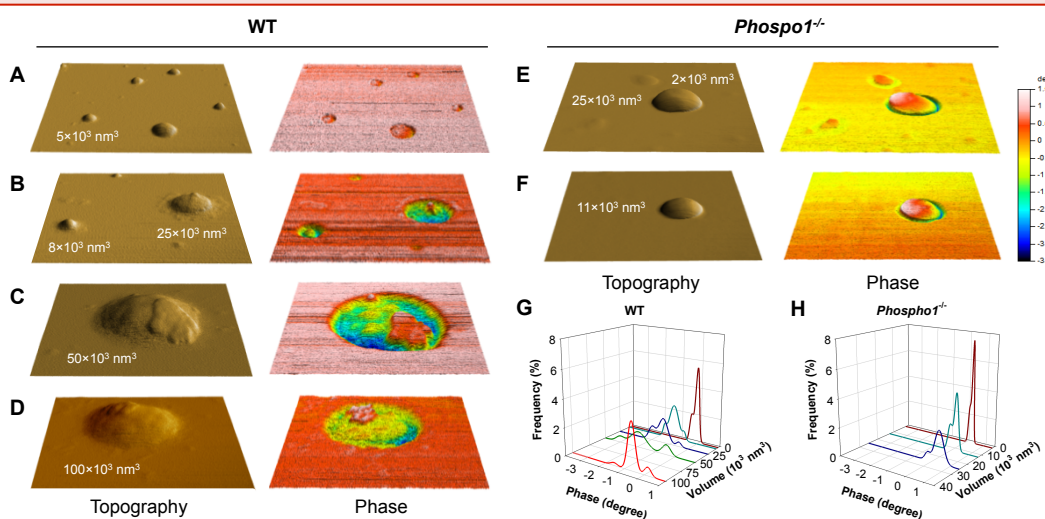


Figure 2. Phase changes with vesicle volume for WT and *Phospho1*^{-/-} MVs. A – F. 3D topography and phase images of WT (A. to D.) and *Phospho1*^{-/-} (E. and F.) MVs with different volumes. Scan size $1 \mu\text{m} \times 1 \mu\text{m}$ (A), $600 \text{ nm} \times 600 \text{ nm}$ (B), $350 \text{ nm} \times 350 \text{ nm}$ (C–F). Phase scale bar on the right is common for all the depicted phase images. G and H. 3D graphs of the distributions of phase values for WT (G) and *Phospho1*^{-/-} (H) MVs represented in the AFM images on the left. These graphs show the changes in lumen viscoelasticity of WT and *Phospho1*^{-/-} MVs with vesicle volume. The distributions of phase values across MV surface were calculated by considering the average phase value of mica substrate equal to zero.

Acknowledgements. This study was supported by grants R01 AR53102 and P01 AG007996 from the National Institute of Arthritis, Musculoskeletal and Skin Diseases (NIAMS), National Institutes of Health (NIH), USA. CF was supported by grant BB/J004316/1 from the Biotechnology and Biological Sciences Research Council (BBSRC), UK.

Disclosure. All authors report no conflicts of interest

REFERENCES

- Wuthier RE, Lipscomb GF. Matrix vesicles: structure, composition, formation and function in calcification. *Front Biosci* 2011; **16**: 2812-902.
- Warner GP, Hubbard HL, Lloyd GC, Wuthier RE. 32P_i and Ca metabolism by matrix vesicles prepared from chicken epiphyseal cartilage microsomes by isotonic Percoll density-gradient fractionation. *Calcif Tissue Int* 1983; **35**: 327-38.
- Yadav MC, Bottini M, Cory E, Bhattacharya K, et al. Skeletal mineralization deficits and impaired biogenesis and function of chondrocyte-derived matrix vesicles in *Phospho1*^{-/-} and *Phospho1/Pit1* double knockout mice. *J Bone Miner Res* 2016. [Epub ahead of print].